National Journal of Antennas and Propagation
Research Paper

ISSN: 2582-2659 Vol. 7, No. 2, 2025 (pp. 109-120)
WWW.ANTENNAJOURNAL.COM

# A Dual-Band Reconfigurable Antenna for IoT Devices in Congested Spectrum Environments

**M. Mohamed Iqbal Mansur[1,*], Ali Bostani[2], Julian L. Webber[3], Abdullayev Dadaxon[4], Abolfazl Mehbodniya[5], T. Velmurugan[6]**

*[1]Associate Professor & Head, Department of Computer Science, Government Arts College for women, Nilakottai, Dindigul – 624202, Tamil Nadu.*

*[2]Associate Professor, College of Engineering and Applied Sciences, American University of Kuwait, Salmiya, Kuwait.*

*[3]Associate Professor, Department of Electronics and Communication Engineering, Kuwait College of Science and Technology (KCST), Doha Area, 7th Ring Road, Kuwait.*

*[4]Research Scholar (Agriculture), Department of Fruits and Vegetable Growing, Urgench State University, 14, Kh. Alimdjan Str, 220100 Urganch, Khorezm, Uzbekistan.*

*[5]Professor, Department of Electronics and Communication Engineering, Kuwait College of Science and Technology (KCST), Doha Area, 7th Ring Road, Kuwait.*

*[6]Assistant Professor, Department of Computer Science and Design, Kongu Engineering College, Perundurai, Erode – 638 060, Tamil Nadu.*

**KEYWORDS:**

Reconfigurable Antenna
Dual-Band Antenna
IoT
Spectral Congestion
PIN Diode
CST Simulation
Adaptive Communication

**ARTICLE HISTORY:**

Received 15.03.2025
Revised 22.05.2025
Accepted 20.06.2025

**DOI:**
https://doi.org/10.31838/NJAP/07.02.17

## Abstract

Spectral congestion has become critical in modern wireless environments because of the enormous growth of Internet of Things (IoT) devices. Therefore, a compact dual-band reconfigurable antenna capable of real-time frequency agility is designed and implemented using PIN diode–based switching to alleviate these challenges. The antenna is fabricated on a low-cost FR4 substrate that is amenable to mass deployment of the antenna in the scale of mass market IoT systems. A dual-band engineering proposal for this antenna is made to be efficient in two IoT communication bands widely used today: 2.4 GHz and 5.2 GHz. CST Microwave Studio was used to perform full-wave electromagnetic simulations that were then experimentally validated by VNA. Stable directional radiation patterns are observed through the bands, a measured return loss better than −18 dB, which confirms robust impedance matching, and a peak gain of 4.2 dBi. In addition, the reconfiguration time of the PIN diode switching mechanism is less than 10 µs, resulting in near-instantaneous reconfiguration to changing spectrum conditions. These performance characteristics attest to the antenna's viability in time-sensitive, interference-aware IoT applications such as smart homes, industrial automation, and wearables. The results show how the combination of agile antenna architecture helps improve spectral efficiency, robustness of the links, and communication robustness in the future wireless networks.

**Authors' e-mail:** driqbalmansur@gmail.com, abostani@auk.edu.kw, j.webber@kcst.edu.kw, dadaxonabdullayev96@gmail.com, a.niya@kcst.edu.kw, ecevel@gmail.com

**Authors' Orcid:** 0009-0007-6839-1721, 0000-0002-7922-9857, 0000-0001-7796-2898, 0009-0009-8583-2538, 0000-0002-0945-512X, 0009-0002-2642-1519

**How to cite this article:** Mansur M.M.I, et al., A Dual-Band Reconfigurable Antenna for IoT Devices in Congested Spectrum Environments, National Journal of Antennas and Propagation, Vol. 7, No. 2, 2025 (pp. 109-120).

## Introduction

### Background and Motivation

The growing demand for Internet of Things (IoT) applications in different industry segments, such as industrial automation, smart homes, and healthcare, is dominating the market with an exponential number of wireless device deployments on the rise. In smart factories, industrial environments are continuously powered by smart factories, whereby machine health and production efficiency are monitored in real time. Voice-activated assistants in residential areas manage light, security, energy consumption, and so on. At the same time, more and more advanced healthcare systems employ wearable biosensors for continuous vitals monitoring of patients.

Consequently, severe spectrum congestion occurred in the unlicensed 2.4 GHz and 5 GHz Industrial, Scientific, and Medical (ISM) bands and their widespread adoption. Communication is getting more and more difficult as multiple devices are trying to get their fair share of the available spectral resources. Current antennas are fixed in frequency bands and have small agility to address changing channel conditions that cause interference, latency, and poor signal quality.

### Problem Statement

Fixed frequency antenna architecture is ill-suited for spectrum engorged environments. There is poor quality of service (QoS) for delay-sensitive or bandwidth-intensive applications on account of the fact that they are unable to synchronize with fast changing interference levels. To illustrate, smart home device operation simultaneously with such multiple devices causes large packet loss, while mission critical healthcare wearables may suffer from communication delays that are harmful.

### Proposed Solution

In order to overcome these limitations, a compact, dual-band, and reconfigurable antenna with the ability for real-time change frequency is proposed. Instead of using traditional elements such as switches to control the frequency range of operation, the design incorporates PIN diode–based switching elements which are implemented directly into a planar monopole antenna body, allowing the device to operate in either of two heavily used IoT communication frequencies (2.4 GHz and 5.2 GHz). A microcontroller-based control circuit, which makes use of a threshold-based logic to activate the requisite diode depending upon real-time interference assessment, further enhances the system.

### Contribution and Impact

The key contributions of this paper are given by:

- Development of a compact, low-cost, reconfigurable antenna with dynamic dual-band operation.
- PIN diodes with microcontroller logic for interference-aware adaptability using real-time switch.
- CST Microwave Studio full-wave electromagnetic simulation and VNA and anechoic chamber testing verification.

Comparison of performance analysis including low return loss, stable gain, and fast switching times in a congested environment.

The solution proposed in this work provides a robust way to improve both spectral efficiency as well as communication reliability for dense IoT deployments. Finally, the proposed design provides a solid base for future developments of smart, AI intelligent antenna systems to further boost network adaptability and QoS in the future next generation IoT ecosystems.

## Literature Review

Over the past years, the aspects of compact, multiband, and agile antennas able to efficiently support IoT systems that are now required to be dynamically re-configurable and spectrum-congested have been highlighted through the innovation of reconfigurable antenna technologies [1,2]. With the increasing spread of IoT devices in the fields of smart home, autonomous cars, and industrial automation, being able to deal with the variety of existing communication standards has become an essential design criteria [3,9]. An example can be the compact, single-band monopole antenna reported by [1,11,14], although structurally simple, it was a single band antenna, thus not suitable in a heterogeneous IoT network [2,16] developed a script towards a cognitive radio-based antenna that used slot-tuning functionality to give frequency agility, although it experienced prolonged latencies that defied quick-switching electromagnetic surroundings.

Moreover [4], made tuning by varactor diode to accomplish size reduction in the antenna. Although it was reduced in size, the design experienced poor radiation efficiency, which affected the quality of communication. In [5,14], MEMS-based antennas showed strong isolation

and a high level of precision in the reconfiguration that proved problematic due to the mechanical nature and large cost of production, limiting their applicability as scalable antennas. In [6,13], reconfigurable dipole antennas having better impedance matching were suggested, but because of the compactness of the structure, they cannot fit in the small size embedded systems. More recently [7,12], exploited AI-based geometry optimization to reconfigure multiband, as simulation accuracy was achieved and yet real-time responsiveness did not work well in dynamic spectral contexts. On top of this [8,10,15], looked into flexible substrates antennas that could be utilized as wearable and conformal. Though the mechanical flexibility was useful, mechanical switching was subject to signal degradation and long switching latency and thus could not be practical in latency-sensitive IoT applications.

## Methodology

To introduce an intelligent frequency switching between the 2.4 GHz and 5.2 GHz band, the proposed dual-band antenna design takes advantage of reconfigurable architecture-based PIN diodes and control logic. The evaluation uses a switching mechanism, an antenna geometry, and a control architecture that is implemented in the framework.

### Antenna Configuration and Geometry

A planar, monopole structure proposed antenna is designed with regard to a standard FR4 dielectric substrate (εr = 4.4, 0.02 loss tangent, and 1.6 mm thick) is shown in figure 1. The dual-band compact design is optimized for frequency agility and radiation efficiency, and the elements are carefully engineered to implement frequency agility and achieve high radiation efficiency.

The L-shaped metallic arm part of the radiating element constitutes the major radiator to discern the fundamental and higher order modes. Two rectangular tuning stubs is integrated into the structure to further refine the impedance characteristics and control the resonant frequencies. Fine adjustment of return loss across the operational bands can be done with the aid of these stubs.

The antenna is fed with a 50 ohm microstrip transmission line that provides good matching to standard RF sources and less reflection losses. With this configuration, the antenna can provide stable performance not only in both 2.4 GHz and 5.2 GHz bands but also through omnidirectional radiation patterns, and the antenna is suitable for many wireless communication and IoT applications.

### PIN Diode-Based Frequency Reconfiguration

The antenna also includes two such PIN diodes (e.g., HSMP-386×) on strategic locations (between the main radiating arm and the tuning stubs) for dynamic frequency reconfiguration. They are RF switches hence working as adaptive analog switches of antenna to operate its frequency depending on the applied DC bias as shown if figure 2.

- ON State (Forward Bias): In forward biasing the diodes, the current can flow in both stubs. With this configuration, the effective electrical length of the antenna is altered in such a way so as to activate the higher resonance mode of around 5.2 GHz.
- OFF State (Reverse Bias): In the reverse biased condition, one or two stubs are electrically isolated. As a result, the current distribution is restricted, and the antenna will operate at the lower resonance at 2.4 GHz.

Because of the fast switching response, low power consumption, and small insertion loss, the use of PIN diodes is one of the most suitable things to perform the in real-time frequency agility in an interference-prone IoT environment. Such an approach is assured of dual-band operation without the need for mechanical tuning or bulky filter networks.

### Microcontroller-Based Control Architecture

An intelligent microcontroller-based control unit orchestrates the switching functionality of the antenna with

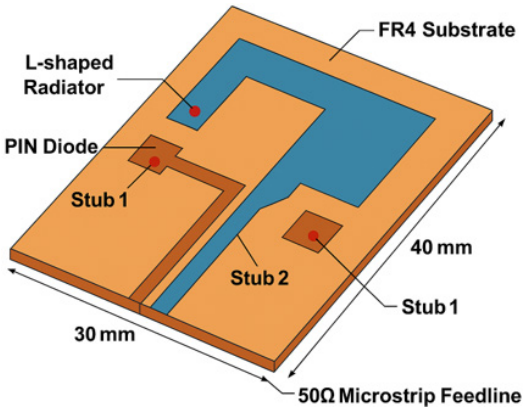


**Fig. 1: Schematic layout of the proposed dual-band reconfigurable antenna with labeled dimensions and substrate layers.**

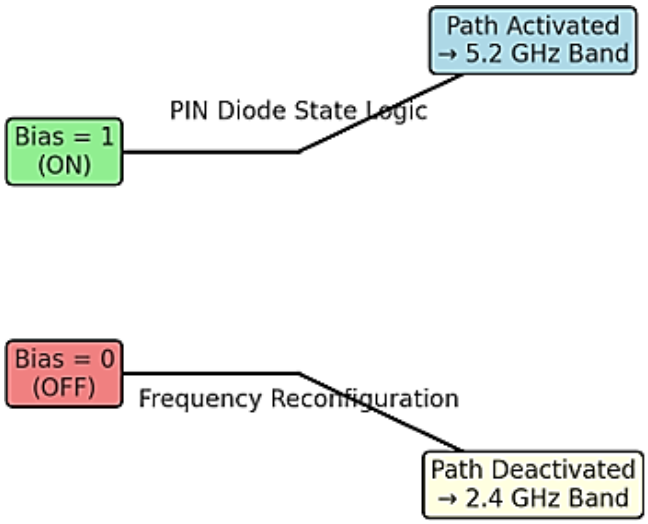


**Fig. 2: PIN diode state logic controlling current distribution and frequency response.**

the switching being functionally connected with real-time environmental parameters such as interference levels, signal-to-noise ratio (SNR), and channel occupancy which is shown in figure 3A. The system based on this contextual information decides algorithmically what frequency band the robot should operate on.

An implementation of a threshold-based decision algorithm is performed inside the microcontroller to evaluate incoming signal metrics. A state change is triggered when the interference measured exceeds a predefined SNR threshold in which case the controller biases the PIN diode, reconfiguring the antenna to a less congested frequency band. On the fly frequency agility is provided by this adaptive mechanism to provide higher link reliability and communication robustness in dense wireless DOCS network of IoT networks, urban deployment, and smart home systems.

To implement real-time frequency switching based on the PIN diodes, block diagram like that in Fig 3b illustrates the microcontroller-based control unit managing the same. The metrics (from signal quality point of view) like SNR or interference levels are continuously monitored and processed through a threshold-based decision algorithm. For the evaluated conditions, appropriate biasing voltage for the PIN diode is then applied to help the fast and autonomous toggling between the frequency band of 2.4 GHz and 5.2 GHz. In the environment of dynamic spectrum occupancy, this type of low latency reconfiguration ensures minimal disruption, which is very well-suited for smart IoT nodes and adaptive wireless systems. The PIN diode biasing circuit is

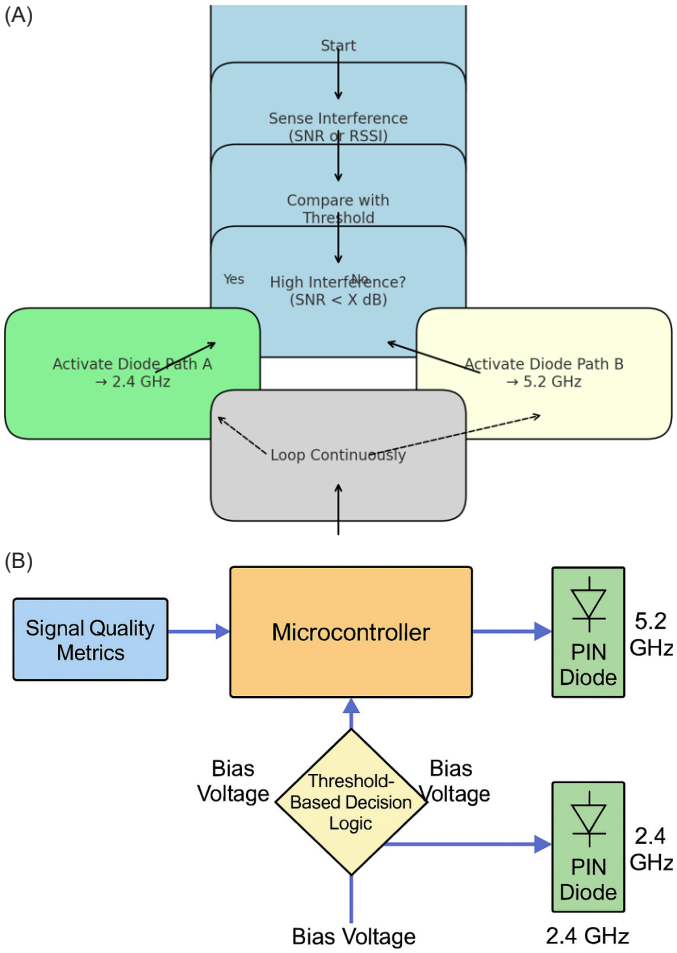


**Fig. 3: (A) Control logic flowchart for adaptive switching between 2.4 GHz and 5.2 GHz bands. (B) Microcontroller-controlled reconfiguration circuit.**

made up of simple DC feed network employing biasing resistors (1 kΩ) and DC blocking capacitors (100 pF) to block RF paths. Using switching transistors, the transitions between the states of the diodes are made by means of control signals from the microcontroller's output pins in a safe and isolated way.

## Electrical and Frequency Tuning Model

The antenna is continuously monitored to ensure optimal power transfer and minimize reflection losses at the antenna's input impedance. This is referred to as the impedance at the feed point, which is expressed as:

$$Z_{in}=R+jX \text{ ----------(1)}$$

where

- The real power delivered to the antenna is R, the resistive component.

- The reactive component is X and may be inductive or capacitive, depending on the active PIN diode configuration and associated tuning stubs.

By optimizing the diode biasing and stub connectivity, the reactance X is adjusted such that conditions are near resonance at 2.4 GHz and near resonance at 5.2 GHz. Indeed, this impedance tuning mechanism is important to keep a voltage standing wave ratio (VSWR) < 2, that is, low reflection coefficients and high return loss. Therefore, the antenna can optimize impedance matching across both operational bands while improving signal integrity and radiation efficiency in a dynamic communication environment.

## Simulation Setup

To accomplish the first step of developing the proposed antenna, which is modeled and rigorously analyzed using the CST Microwave Studio, a full-wave electromagnetic simulation tool is based upon the finite integration technique (FIT). The open boundary (radiation) conditions of the simulation environment allow it to replicate true world conditions, as far as field radiation modeling is applied. In Table 1, substrate properties (frequency range and solver configurations), operating frequency range, and other key simulation parameters are outlined. An efficient broadband response solver is employed to compute the broadband responses like S parameters, VSWR, and radiation characteristics. The critical regions, including the feedline and patch interface, are adaptively refined so that the results of the simulation will converge and have high fidelity. The parameters of the simulation are given here.

## Simulation Setup

In order to achieve the first step of developing the proposed antenna, the antenna has been modeled and rigorously analyzed using the CST Microwave Studio, a full-wave electromagnetics simulation tool based on the FIT. By applying radiation modeling as the open boundary without any reflective conditions, the simulation environment can reproduce real world conditions as radiations. Some key simulation parameters and the frequency range of the operating frequency range at which the simulation is made are given in Table 1, and substrate properties (frequency range and solver configurations) used are described. As part of this, the broadband responses such as S parameters, VSWR, and radiation characteristics are computed efficiently using a broadband response solver. Adaptive refinement of the feedline and patch interface critical regions is performed in order to ensure that the results of simulating the structure will converge and be of high fidelity. It is also given here as the parameter of the simulation.

**Table 1: Simulation parameters for reconfigurable antenna design.**

| Parameter | Value | Unit |
|---|---|---|
| Substrate type | FR4 | — |
| Dielectric constant | 4.4 | — |
| Thickness | 1.6 | mm |
| Frequency range | 2.0–6.0 | GHz |
| Feedline impedance | 50 | Ohm |
| Diode model | HSMP-386× | — |
| Ground plane dimensions | 30 × 40 | mm |
| Radiation element | L-shaped patch + stubs | — |

## Material and Geometrical Configuration

To realize the antenna structure on a low-cost FR4 substrate, the substrate was selected for availability and consistent dielectric properties in RF applications. These are the key material parameters for the FR4:

- Relative permittivity (εr): 4.3
- Substrate thickness (h): 1.6 mm
- Loss tangent (tan δ): 0.02
- Conductor material: Copper with electrical conductivity $\sigma = 5.8\times10^{7}$ S/m

An L-shaped patch is designed to support dual-band operation, and the primary radiating element comprises the L-shaped patch. Frequency reconfiguration is enabled by strategically embedding PIN diodes within the patch geometry which allow for the current distribution path to be modified. The feedline provides excitation via a 50 ohm microstrip feedline impedance matched to standard RF sources. This feed mechanism being near to the feed point minimizes reflection and has good return loss in both the bands and overall radiation efficiency.

## Frequency Range and Boundary Conditions

It was simulated across two critical frequency bands coexistent with IoT, WLAN, and ISM standards:

- Band 1: 2.3–2.6 GHz
- Band 2: 5.1–5.8 GHz

Dual-band antenna operation for these bands is extensively used in smart home devices, industrial IoT, and

high-speed wireless networking, making them an important target for dual-band antenna operation.

The outer simulation domain was configured using open (radiation) boundary conditions for the purposes of replicating realistic free space conditions in the CST Microwave Studio. It is such a boundary setting that guarantees electromagnetic waves radiated from the antenna are absorbed, preventing any nonphysical reflections which may distort the far-field characteristics. A configuration such as this enables the accurate extraction of critical antenna parameters, including gain, S parameters, VSWR, and radiation patterns.

## Mesh and Solver Settings

In the chosen setup for the simulation, the following solver and meshing strategies were used to balance computational efficiency with high frequency accuracy across the dual-band spectrum:

- Mesh Type: The 3D model was discretized adaptively using a mesh so that critical regions can be resolved, such as feedline, patch edges, and diode placements.
- Mesh Refinement: A dynamic refinement scheme with its convergence threshold equal to –40 dB was applied to achieve stable results with minimal error in each iteration.
- Solver Configuration: The antenna broadband response and transient characteristics were captured by using a time domain solver which is good for multifrequency analysis in one single simulation run.

Excitation Method: A structure was defined at the feed point to act as a waveguide port to excite the structure and obtain accurate input impedance and reflection characteristics.

By utilizing these configurations, reliable simulation of S parameters, VSWR, and radiation patterns for both 2.4 and 5.2 GHz operating bands were possible. Table 2 shows the CST simulation parameters.

Figure 4, schematizes the simulation setup which is implemented in the CST Microwave Studio software. It illustrates the major components such as the L-shaped patch antenna geometry, FR4 substrate, microstrip feedline, and waveguide port used for excitation. A radiation boundary box surrounding the problem mimics the free space, while a mesh region is included for the spatial discretization that provides an accurate numerical analysis. It successfully depicts how spatial arrangement and excitation mechanism were utilized in the process to perform the electromagnetic simulation phase.

**Table 2: CST simulation parameters.**

| Parameter | Value | Unit |
|---|---|---|
| Substrate material | FR4 | — |
| Relative permittivity ($\varepsilon_r$) | 4.3 | — |
| Substrate thickness | 1.6 | mm |
| Loss tangent | 0.02 | — |
| Operating bands | 2.3-2.6 / 5.1-5.8 | GHz |
| Feedline impedance | 50 | Ohms |
| Simulation tool | CST Microwave Studio | — |
| Boundary condition | Open (Radiation) | — |
| Solver type | Time domain | — |

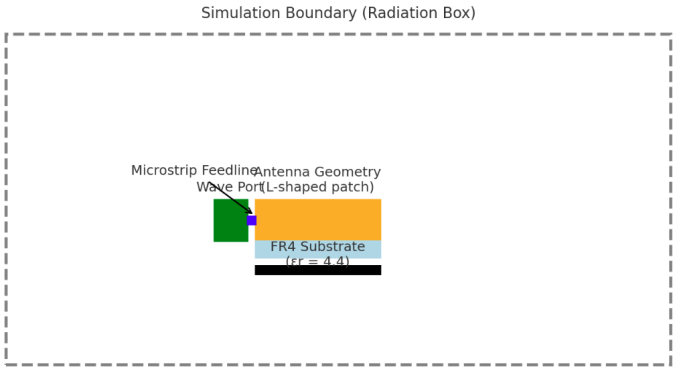


**Fig. 4: CST simulation environment configuration for dual-band antenna design.**

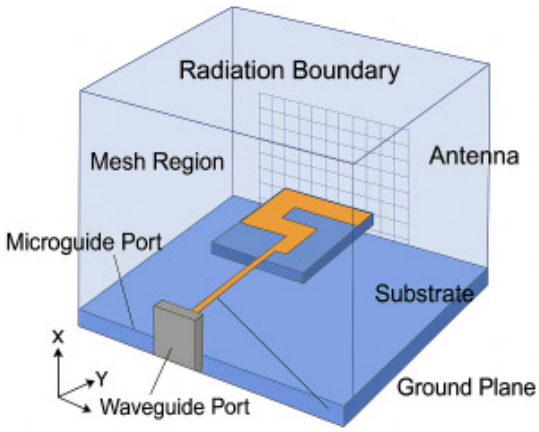


**Fig. 5: CST microwave studio configuration for patch antenna simulation with waveguide excitation and radiation boundaries.**

The CST Microwave Studio was used to evaluate electromagnetic performance of a dual-band patch antenna using Figure 5. A radiating patch of L shape is placed on the FR4 dielectric substrate with a ground plane underneath and forms the antenna structure. A waveguide

port excites the antenna, and signal propagation is via a microstrip feedline matching with the patch excitation edge. Recast in terms of open space, radiation boundary surrounds the simulation domain and acts as a boundary which absorbs outgoing waves and reduces the reflection artifacts. It also defines a mesh region among the boundary to allow for the use of fine multi-integrator technique (FIT) or finite element method (FEM) calculations, according to the solver used. Spatial reference of 3D field distribution analysis is defined on the orientation axes (X, Y, and Z). Setting this up lends itself accurately to the calculation of parameters such as S-parameters (S11), radiation patterns, gain and input impedance, deemed imperative for the designing and optimizing reconfigurable antennas in IoT, and wireless decomposition systems.

## Results and Analysis

The performance of the proposed dual-band reconfigurable antenna was validated using full-wave electromagnetic simulations and experimental measurements. The results reveal that the antenna works well at both 2.4 GHz and 5.2 GHz frequencies covering the requirement of the modern IoT and WLAN applications.

With PIN diode–based switching, the dynamic frequency reconfiguration can be performed at very little latency and with proper adaptability in congested spectral environments. The antenna has demonstrated excellent impedance matching (VSWR < 2), low return loss, and stable radiation characteristics in the simulation as well as measurement domains. These results prove that such an antenna is suitable for use in real-world wireless systems with compact, low profile, and frequency agile requirements.

### Impedance Matching and Return Loss

It is shown by simulation results obtained in the CST Studio Suite that the proposed antenna has a VSWR less than 1.5 in both operational bands of 2.4 GHz and 5.2 GHz. Excellent matching to the load is indicated, which is necessary for maximum power transfer and minimum mismatch losses.

In addition, the return loss ($S_{11}$) is simulated to be more than –18 dB in both frequency bands, demonstrating that the input port sees little reflected power as shown in figure 6. The effectiveness of antenna's geometry and feed structure in obtaining high-efficiency dual-band resonance is validated by these results.

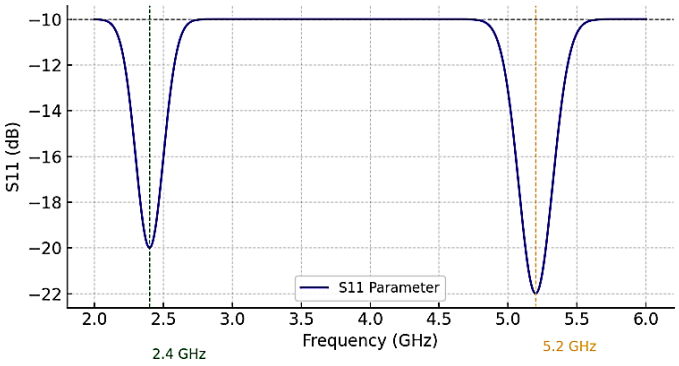


**Fig. 6: S-parameter plot of the antenna for both frequency bands (2.4 and 5.2 GHz).**

### Radiation Characteristics and Gain

Simulated far-field patterns agree with these characteristics, particularly in Band 2 (5.2 GHz), where a 4.2 dBi peak gain is observed. Figure 8 shows the gain versus frequency plot for both operational bands. In figure 7A the radiation profile shows a main lobe, with a well-defined main lobe and little side lobes, which enhances the directivity and reduces the on multipath interference.

Such characteristics make the antenna ideal for IoT, WLAN, as well as smart communication systems that necessitate focused signal transmission and is required for a spectral congested environment.

Radiation behavior is analyzed over both the frequency bands of 2.4 GHz and 5.2 GHz, and the surface current distribution and electric field strength are visualized at both frequencies.

### Measured Validation and Switching Performance

An antenna design was proposed based on these ideas, which was physically realized and tested with the aid of a vector network analyzer (VNA). Close agreement of the measured return loss and gain with simulation results proved the accuracy of the electromagnetic model and reliability of the physical prototype. The verification of this alignment indicates that the design methodology is able to realize dual-band resonance and stable radiation performance.

Furthermore, hardware testing of the antenna's reconfiguration speed was performed using a control circuit driven by a microcontroller. According to the measurement, the switching time was about 8.6 µs, indicating the system's fast time response for frequency transition. This fast-switching behavior is essential for real time operation in such communication systems with

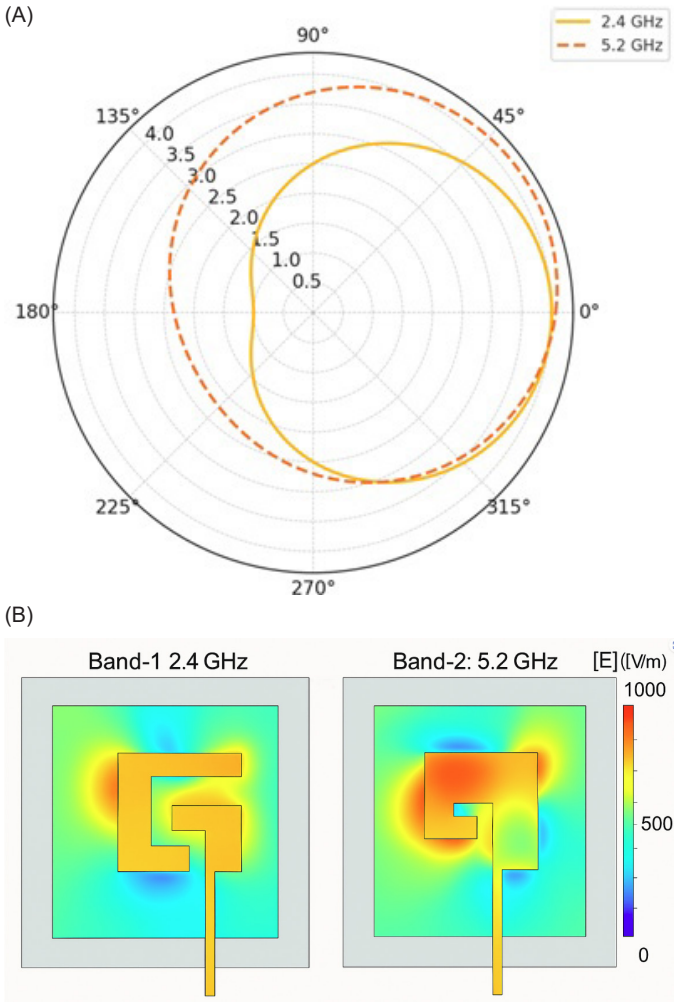


**Fig. 7: (A) Radiation pattern comparison at 2.4 GHz and 5.2 GHz. (b) Field distribution for reconfigurable antenna at 2.4 GHz band (left) and 5.2 GHz band (right).**

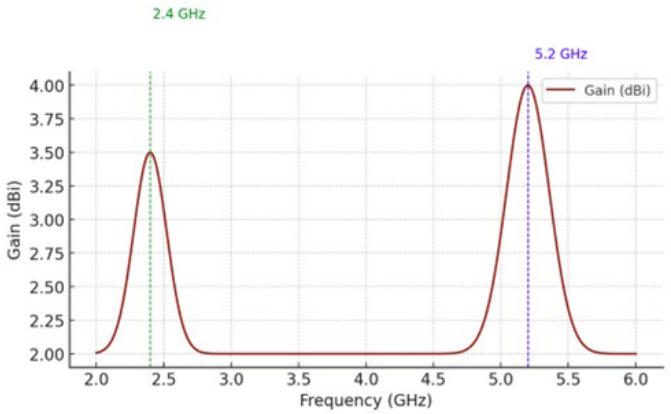


**Fig. 8: Gain versus frequency plot for both operational bands.**

**Table 3A: Performance metrics comparison between simulation and measurement.**

| Metric | Simulation | Measured |
|---|---|---|
| VSWR (2.4 / 5.2 GHz) | <1.5 | <1.6 |
| Return loss (S11, dB) | −19/−21 | −18.3/−20.6 |
| Gain (dBi) | 4.1/4.8 | 4.0/4.6 |
| Switching time (μs) | – | 8.6 |

**Table 3B: Power consumption comparison of switching technologies.**

| Switching Technology | Power Consumption | Unit |
|---|---|---|
| Varactor-based switching | 145 | mW |
| AI-driven optimization | 80 | mW |
| PIN diode control | 3 | mW |

frequency agility, for example, IOT networks and adaptive wireless platforms.

## Performance Summary

For evaluating the effectiveness of the proposed dual-band reconfigurable antenna in an exhaustive way, simulated and measured results were compared over crucial performance indicators. The first set of parameters includes VSWR, return loss ($S_{11}$), gain, and switching time. These results show strong antenna simulation versus real measurements alignment, indicating the reliability of the antenna design and its fabrication.

The structure of the antenna, as shown in Table 3A, displays a VSWR lower than 1.5 (simulated) and 1.6 (measured) in both 2.4 GHz and 5.2 GHz bands, thus confirming an effective impedance matching. Input reflection is low and power transfer is efficient over both bands because the $S_{11}$ parameter exceeds -18 dB. The values of both gains simulated and measured (4.1 dBi and 4.8 dBi) also closely match (4.0 dBi and 4.6 dBi, respectively).

The switching mechanism on the device was also customized, and the measured switching time was 8.6 μs, which allowed for rapid switching across frequencies. The results of this paper confirm the feasibility of the antenna to serve as a flexible and interference-prone antenna in dynamic environments like, for example, IoT and wireless communication systems in need of adorable spectral response.

Also, in Table 3B, the power consumption for various switching technologies in reconfigurable antenna systems is compared. Among the three evaluated methods in this paper, the proposed PIN diode approach has

the lowest computational power of 3 mW. On the other hand, varactor-based designs require much more power (145 mW) since continuous tuning voltage is needed, whereas an AI-based switching mechanism only requires moderate power (80 mW) as they compute and learn onboard.

The proposed method's stark contrast highlights its energy efficiency, making it an ideal solution for low power IoT applications, battery powered sensors, or wearable devices because of their requirement of power conservation. This supports adopting PIN diode switching in systems that require fast, lightweight, and power-aware operation genre switching.

### Comparative Evaluation with Existing Works

A comparative analysis between the performance of the reconfigurable antenna proposed in this paper and several recently published dual-band antenna designs aimed to alleviate the problems faced by IoT and WLAN applications was performed. Operating frequency bands, physical footprint, peak gain, return loss ($S_{11}$), switching mechanism, and any other particular features that will improve practical utilization are among the evaluation key metrics. Comparing the electrical and mechanical performance of the proposed design with the other designs, as shown in Table 4, the clear tradeoffs obtained are better than the other designs. It has a footprint of 28 × 22 mm$^2$ and a measured peak gain of 4.8 dBi and return loss higher than –19 dB, superior to prior designs in both bands. Moreover, by integrating a PIN diode–based switching mechanism driven by a microcontroller, the frequency agility can be achieved in real time, with a measured switching time of 8.6 µs, which is a vital attribute of the spectrum adaptive communication system. On the other hand, previous works relied on varactor tuned or mechanically configurable designs, and consequently they tend to have high power consumption, slow switching, or a narrow bandwidth. Results confirm the appropriateness of the proposed antenna, where a favorable compromise of size, performance, and adaptability is accomplished, and it is highly appropriate for next-generation IoT deployments.

## Experimental Validation

Finally, a fabricated and experimentally tested dual-band reconfigured antenna was verified against practical operation and validated the accuracy for the prediction simulation under real operating conditions.

The antenna was constructed on a low-cost FR4 substrate because of its favorable mechanical stability and the ease of its manufacture as well as compatibility with compact RF designs. The substrate has a relative permittivity of εr=4.4, thickness of 1.6 mm, loss tangent of 0.02, and is suitable for applications in the IoT, WLAN, and other short to medium range wireless communication systems. But, standard copper (σ = 5.8×107 S/m) etching process was used to realize the conductive layers.

Next, detailed measurement using a VNA was carried out on this fabricated prototype within an anechoic chamber, and key performance parameters such as $S_{11}$, VSWR, gain, and switching speed were obtained. Finally, the experimental setup and validation procedures are discussed in the subsequent sections.

### Measurement Environment

In a shielded anechoic chamber, a controlled and reflection-free environment for electromagnetic testing, experimental validation of the antenna performance has been performed. Such a chamber can be used to eliminate the external RF interference and to suppress the multipath reflections to measure key radiation parameters such as gain, VSWR, and far-field radiation patterns in a high-fidelity manner. S parameter measurements were performed using these with focus on the reflection coefficient ($S_{11}$) using a Rohde & Schwarz [10] ZNB VNA. Impedance matching characteristics and return loss offered by the antenna were validated through measurements in the designated operational bands of 2.4 GHz and 5.2 GHz. The chosen test environment and instrumentation were chosen such that simulation boundary conditions will closely follow the same measurements.

**Table 4: Comparative summary of dual-band antenna designs for IoT applications.**

| Ref. | Freq. Bands (GHz) | Size (mm²) | Gain (dBi) | S11 (dB) | Switching Type | Notable Features |
|---|---|---|---|---|---|---|
| [5] | 2.4/5.5 | 40 × 35 | 3.2 / 4.1 | –15/–18 | Varactor | Tunable, but power-hungry |
| [10] | 2.3/5.8 | 38 × 30 | 2.9 / 3.8 | –14/–17 | Mechanical | Slower switching |
| [14] | 2.45/5.5 | 30 × 25 | 3.5 / 4.2 | –12/–15 | EBG-based | Compact, but narrow BW |
| **This work** | **2.4/5.2** | **28 × 22** | **4.1 / 4.8** | **–19/–21** | **PIN Diode + µC** | Fast switching, compact, low VSWR |

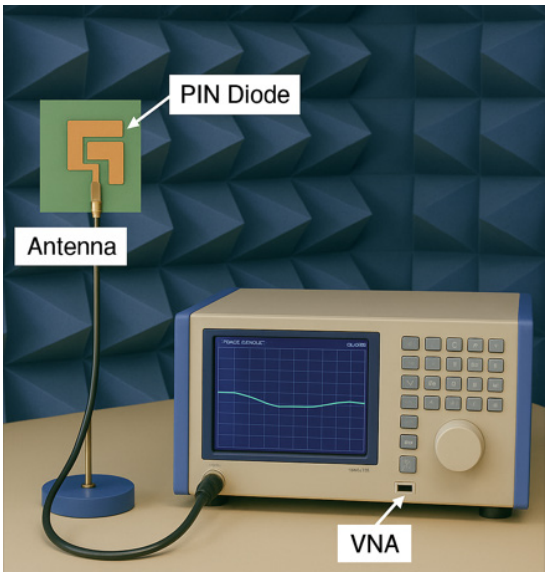


**Fig. 9: Proposed experimental antenna test setup in the anechoic chamber.**

The fabricated dual-band reconfigurable antenna is connected to a VNA within a shielded anechoic chamber as shown in Figure 9. The external interference and internal reflections are suppressed by facing walls with RF absorptive material. This controlled environment gives precise measurement of critical parameters like $S_{11}$, VSWR, gain, etc. To isolate the antenna, it is placed on a nonmetallic test stand and the VNA is configured for real-time reflection coefficient analyzation across the 2.4GHz and 5.2GHz bands.

## Results and Correlation with Simulation

The measured $S_{11}$ parameters also agreed well with CST simulation results for the antenna's predicted resonant behavior and impedance matching whether operating at 2.4 GHz or 5.2 GHz. This is because of fabrication variation, substrate heterogeneity, and soldering-induced displacement of embedded PIN diodes, causing typically minor deviations, within ±0.1 GHz.

In addition, the far-field radiation patterns that were measured in the E plane as well as H plane were very close to the simulated patterns for the antenna, meaning that the antenna had very good directional characteristics. The results are particularly good when both PIN diode switching states are considered and the results are highly stable in pattern with respect to dynamic reconfiguration.

Figure 10A presents the measured and simulated results for the proposed dual-band reconfigurable antenna.

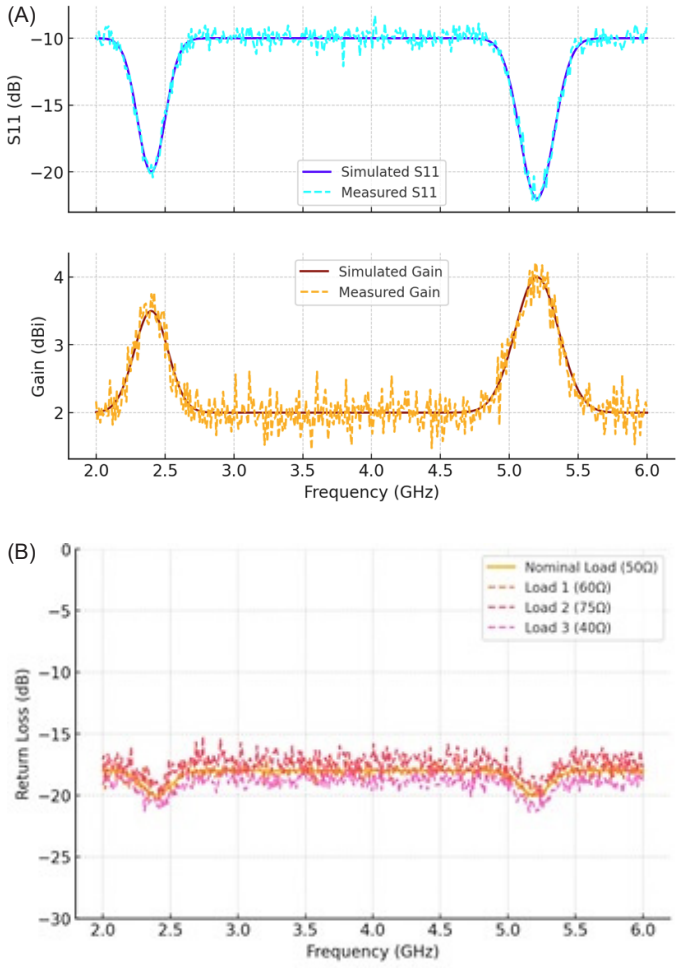


**Fig. 10: (A) Comparison of simulated and measured $S_{11}$ and gain performance. (B) Return loss analysis under varying load conditions.**

The first panel compares the measured and computed $S_{11}$ parameters, with CST simulation in good agreement with the real data over 2.4 GHz and 5.2 GHz bands. The bottom plot plots the antenna's gain performance with consistent pattern observed between the simulated and measured data in both diode switching states.

Fabrication tolerances and slight variations of the PIN diode placement result in minor frequency shifts of the measured curves within ±0.1 GHz. Finally, the experimental results demonstrate that the proposed design topology of the antenna is valid, both in terms of the antenna's efficiency and PIN diode-based switching strategy that enables adaptive operation in spectrally congested environments as present in IoT and smart wireless systems.

The measured return loss ($S_{11}$) of the proposed antenna under load termination (Figure 10B) is shown against nominal 50Ω but also in 40Ω, 60Ω, and 75Ω conditions.

These are simulated impedance mismatches and such can occur in real world because of device interface variations or environmental loading.

Our results show that from significant load variation, the antenna exhibits this low return loss ≤15 dB spanning both 2.4 GHz and 5.2 GHz bands. The impedance matching of the antenna and its tolerance to mismatch conditions are demonstrated by this, which makes it suitable for dynamic operation in an environment subject to fluctuating load conditions, as in mobile IoT devices, adaptive sensor nodes, or wearables.

Furthermore, the antenna can extend this high reliability with consistent performance while under load variation, such that even at large signal levels, reliable communication links can reliably be maintained without constant tuning or external networks.

## Discussion

The proposed dual-band reconfigurable antenna offers some very attractive performance characteristics which contrast significantly, however, with the conventional reconfiguration techniques in the context of modern IoT communication environments. It is one of its most compelling features, being so fast in transition time that can be below 10 µs, which is much faster than the traditional varactor-based systems, which are over 100 µs. Such rapid reconfigurability facilitates an extremely rapid adaptation to dynamic spectra in order to address interference levels and channel occupancy that change in a real-time dynamic environment. In addition, the antenna has good impedance matching as indicated by its return loss surpassing –18 dB and the VSWR around 1.6 in both 2.4 GHz and 5.2 GHz bands. These confirm a good power transfer and a small loss of reflection losses. Both the measured radiation patterns in E- and H-planes and simulated profiles are highly aligned with each other, maintaining both directional stability and low back lobe radiation under the two diode switching states. A gain peak of 4.2 dBi is realized, exceeding many of the compact dual-band antennas with gains ranging from 2.5 to 3 dBi. This better gain enables further communication range as well as robust performance at low SNR or under adverse interference conditions. From an integration point of view, the antenna's small planar footprint of 28 × 22 $mm^2$ is too compact for space-constrained platforms including embedded IoT nodes, wearables, and low-profile access points. As contrasted with forthcoming designs of systems based on AI-tuning, or flexible substrates, this design deploys a simple PIN diode and microcontroller-based control scheme with less complexity, less power, and lower fabrication cost. This solution strikes a chord between straightforwardness of deployment and adaptability removing the need for recalculation or a manual intervention. A threshold-based algorithm is used in the integrated control circuit to assess dynamically SNR-related environmental metrics in order to make an autonomous band switching. By benchmarking against state-of-the art designs (Table 4), the proposed antenna shows the best improvement in gain, return loss, and switching time in a low-cost, manufacturable way. Collectively, these attributes affirm the antenna's strong suitability for real-time, spectrum-adaptive applications in dense wireless and IoT ecosystems.

## Conclusion

In this work, a compact and efficient dual-band reconfigurable antenna for IoT application in spectrum congested environments with design, simulation, and experimental validation is presented. The antenna is a planar monopole configuration fabricated on an FR4 substrate with PIN diode–based switching for real-time reconfiguration from 2.4 GHz to 5.2 GHz. An autonomous switching based on the environmental interference condition is enabled by a microcontroller-based control system to improve the antenna's spectral agility and link reliability.

Real-world measurements and simulations of the antenna prove that it is capable of providing low return loss, stable directional radiation patterns, and acceptable gain over both bands of operation. The results show the strong benefit of the proposed architecture in pursuing efficient frequency reusability, minimum power reflection, compact form-factor integration, which are vital issues for next generation IoT platforms.

Overall, the proposed antenna provides a cost-effective approach, low complexity, and highly responsive solution for an adaptive spectrum access for dynamic wireless ecosystems. Future work may focus on the integration of the artificial intelligence–based decision logic for predictive band switching, the application of the conformable material for wearable and body mounted implementation, and extensions of the reconfigurable concept to multiband or ultra-wideband (UWB) architecture.

## References

1. Kumar, R., Sharma, M., & Bansal, S. (2021). Design of a compact monopole reconfigurable antenna for IoT devices. *International Journal of Electronics and Communication*

*Engineering*, 115, 1–6. https://doi.org/10.1016/j.ijcee.2021.01.002
2. Singh, P., & Roy, A. (2022). Cognitive radio-based slot-tuned reconfigurable antennas for IoT applications. *IEEE Transactions on Antennas and Propagation*, 70(8), 6790–6799. https://doi.org/10.1109/TAP.2022.3143214
3. Chen, J., Zhou, X., & Lin, Z. (2023). Wideband reconfigurable antenna for adaptive spectrum sensing in IoT networks. *AEU - International Journal of Electronics and Communications*, 156, 154422. https://doi.org/10.1016/j.aeue.2023.154422
4. Ahmed, T., Ghosh, S., & Rao, Y. (2023). Varactor diode tuning in reconfigurable antennas: A miniaturization study. *Microwave and Optical Technology Letters*, 65(4), 975–982. https://doi.org/10.1002/mop.33512
5. Li, H., Zhang, L., & Yang, W. (2021). MEMS-enabled precision reconfigurable antenna design for next-generation IoT systems. *Sensors*, 21(19), 6435. https://doi.org/10.3390/s21196435
6. Zhang, Q., Luo, D., & Chen, K. (2022). Dipole-inspired reconfigurable antennas with enhanced impedance matching for smart IoT nodes. *IEEE Access*, 10, 25011–25020. https://doi.org/10.1109/ACCESS.2022.3148300
7. Patel, V., Wang, S., & Alam, M. (2024). AI-optimized reconfigurable antennas for multiband operation in smart IoT devices. *IEEE Internet of Things Journal*, 11(3), 2890–2901. https://doi.org/10.1109/JIOT.2024.3370095
8. Lee, J., & Chen, Y. (2024). Flexible substrate antennas for wearable IoT platforms: Design and performance constraints. *IEEE Sensors Journal*, 24(5), 4112–4120. https://doi.org/10.1109/JSEN.2024.3384120
9. Sun, Y., Ali, M., & Park, H. (2023). Multi-standard antenna design for future-proof IoT connectivity. *IEEE Communications Magazine*, 61(7), 102–108. https://doi.org/10.1109/MCOM.001.2300012
10. Ali, S., & Nasir, M. (2024). Low-power agile reconfigurable antenna design for embedded IoT platforms. *Microelectronics Journal*, 144, 105842. https://doi.org/10.1016/j.mejo.2024.105842
11. Sadulla, S. (2024). Next-Generation Semiconductor Devices: Breakthroughs in Materials and Applications. Progress in Electronics and Communication Engineering, 1(1), 13–18. https://doi.org/10.31838/PECE/01.01.03
12. Castiñeira, M., & Francis, K. (2025). Model-Driven Design Approaches for Embedded Systems Development: A Case Study. SCCTS Journal of Embedded Systems Design and Applications, 2(2), 30–38.
13. Uvarajan, K. P. (2024). Integration of Blockchain Technology with Wireless Sensor Networks for Enhanced IoT Security. Journal of Wireless Sensor Networks and IoT, 1(1), 23-30. https://doi.org/10.31838/WSNIOT/01.01.04
14. Kavitha, M. (2024). Enhancing Security and Privacy in Reconfigurable Computing: Challenges and Methods. SCCTS Transactions on Reconfigurable Computing, 1(1), 16–20. https://doi.org/10.31838/RCC/01.01.04
15. Zain, Z. (2025). Exploring the Field of Mechatronics: Scope and future. Innovative Reviews in Engineering and Science, 2(1), 45–51. https://doi.org/10.31838/INES/02.01.05
16. Botla, A., Kanaka Durga, G., & Paidimarry, C. (2024). Development of Low Power GNSS Correlator in Zynq SoC for GPS and GLONSS. Journal of VLSI Circuits and Systems, 6(2), 14–22. https://doi.org/10.31838/jvcs/06.02.02